

BEARING STRENGTH ASSESSMENT OF COMPOSITE MATERIAL THROUGH NUMERICAL MODELS

Euler S. Dias*, Carlos A. Cimini Jr.*

* Federal University of Minas Gerais, Dept. of Structural Engineering, Belo Horizonte - MG - Brasil

Keywords: *bearing; composite; allowable; numerical analysis*

Abstract

The introduction of singularities in a material is followed by changes in its mechanical behavior due to updates imposed in the stress path, which leads to stress concentrations. Composite materials have the capacity to be insensitive to notches until a certain size and, for bigger notches, it progressively loses this ability until the material acquires the characteristic behavior of a fragile material. When the objective is to join a component made of composite material with other parts, the possible methods to do the joint and their particularities should be taken into account, whether adhesive or fastening with rivets and bolts. The strength allowable for a chosen failure mode is a recurrent issue when designing a joint of composite material structures, and some modes are preferable to others for not onsetting a catastrophic failure of the structure. In shear strength analysis, it is preferable to design the component so that the first failure mode be bearing failure, and not shear out or net tension failure. Following this guideline, the structure can redistribute the load between the remaining fasteners and avoid the onset of a catastrophic failure. In this paper, numerical methods are used to preview the bearing strength of composite materials as a tool to avoid excessive experimental testing. For the same composite and joint configuration, a set of simulations applying different failure criteria is employed, starting with more simple and wide known criterion and progressively adopting more complex models and failure criteria to evaluate the mechanical response of the material in bearing load.

1 Introduction

The applicability of composite structures has increased over time extending to technologies besides aeronautics. A very common issue in this material adoption concerns in joint the structures. There are several ways to do a joint, as the most common are rivets, bolts and glue, each one with his own pros and cons.

The joint is a very requested part of the structure, considered as a bottleneck in design process as the load path converged do this region to transfer the load from one part to another. When fasteners is adopted the stress concentration surrounding its location is an issue due to many effects that occur in the composite material, such as fiber cracks, fiber micro-buckling, matrix cracks and delamination. Furthermore, there are others variables related to how the fastening was made, like bolt clearance, washer size, lateral constraint, and clamping force that affects the joint strength.

In this article, the widely adopted failure criteria were used to predict the strength under bearing load for a quasi-isotropic composite setup with load transfer through a pin. Not only the damage progression in the composite material was monitored, but also the mechanical behavior from the numerical simulations was compared to experimental data from literature.

2 Overview of bearing analysis in composites

In summary, the joints would be mostly expected to fail in three modes, namely, net-tension, shearing-out, and bearing (Figure 1). In the design stage, the bearing failure must be the first failure mode, so that the material can fail locally, but still be able to carry additional load, unlike other failure modes that lead to catastrophic failure that can result in unrecoverable losses.

Bearing failure is a local compressive failure mode due to contact and frictional forces acting on the surface of the hole [1].

This fracture process is very complicated and is influenced by many parameters, as it is following mentioned.

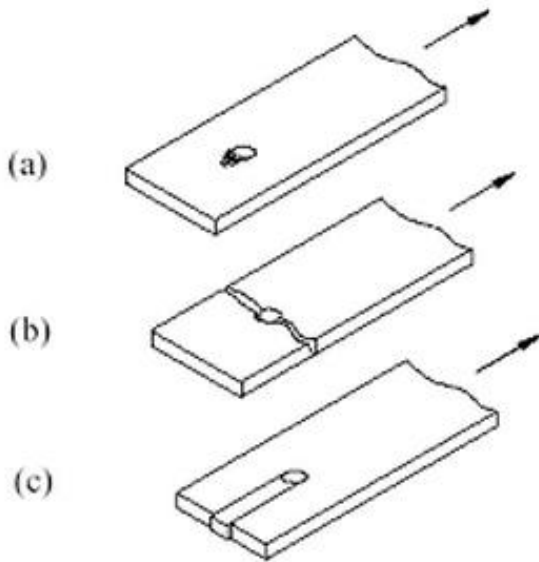


Fig. 1. Failure modes in shear joints: (a) bearing failure, (b) net tension failure, and (c) shear out failure

Fiber micro-buckling, matrix cracks, delamination, and other forms of damage frequently are connected to the 3D failure mode under compressive load in laminated composites [2] [3]. Therefore, an understanding of the occurrence and progress of the microscopic damage is indispensable to the evaluation of the parameters of damage tolerance in structural design.

Fiber micro-buckling and matrix cracking appear to be the dominant modes for the onset of damage, while the final failure stage is dominated by out-of-plane shear cracks and delamination [2]. The lateral constraints and the matrix “toughness” based on the laminate also influence the bearing failure and damage mechanisms.

The effects of fiber-to-load inclination angle and laminate stacking sequence on the bearing load capacity have been determined experimentally on two different type of glass fiber/epoxy laminates: unidirectional and bi-directional (cross-ply) [4].

Experimental results show that composites with three-dimensional woven fiber reinforcement exhibit exceptional strength when subjected to off-axis bearing loads despite the lack of off-axis reinforcement [5].

An approach combining finite element damage analysis and a stochastic technique was adopted to analyze the probabilistic properties for the design-oriented strength of the bolted joints in CFRP laminates [6]. Then a proper value of the fitting factor was proposed instead the common value of 1.15 widely adopted in metallic materials design.

Fiber kinking is one of the main failure modes of composite laminates under compression loading. High-resolution CT showed that kinking is largely involved in the events leading to laminate collapse, notably by triggering other damage modes such as delamination [7]. Kink bands develop extremely progressively, leading to the formation of a wide localization zone, which requires the characteristic behavior of kink bands to be taken into account [7].

Effects of bolt-hole clearance on the stiffness and strength of composite bolted joints were investigated by McCarthy in a single-lap and single-bolt configuration [8]. It was found that increasing clearance was found to result in reduced joint stiffness and increased ultimate strain. A delay in load take-up also occurred with the higher clearance joints, which has implications for load distributions in multi-bolt joints.

Xiao *et al.* [9] used a model to evaluate the local force–displacement responses of a number of single-lap joints installed in a hybrid composite-aluminum wing-like structure subject to bending, twisting and thermal loads. It is shown that the fastener forces caused by the temperature difference are of significant magnitude and should be taken into account in the design of hybrid aircraft structures.

3 Failure criteria

3.1 Maximum Stress failure criterion

The theory of the maximum admissible tension determinates that the failure occurs if at least one of its axial components in one of the main

directions of the material exceeds the corresponding resistance of the respective direction. Regarding the plane stress, the failure occurs if one of the following conditions is satisfied in the ply on-axis direction:

$$\sigma_1 \geq S_{11}^+, \text{ for } \sigma_1 > 0 \quad (1)$$

$$\sigma_1 \leq -S_{11}^-, \text{ for } \sigma_1 < 0 \quad (2)$$

$$\sigma_2 \geq S_{22}^+, \text{ for } \sigma_2 > 0 \quad (3)$$

$$\sigma_2 \leq -S_{22}^-, \text{ for } \sigma_2 < 0 \quad (4)$$

$$|\sigma_{12}| \geq S_{12} \quad (5)$$

where:

S_{11}^+ - longitudinal tensile strength;

S_{11}^- - longitudinal compressive strength;

S_{22}^+ - transverse tensile strength;

S_{22}^- - transverse compressive strength;

S_{12} - in-plane 1-2 shear strength;

The Maximum Stress criterion does not consider the interaction between the stress components.

3.2 Tsai-Wu failure criterion

The failure criterion based on polynomial theory of interactive tensor is capable of predicting the resistance of anisotropic materials under any state of stress. This criterion uses the concept of stress tensors, which allows the transformation between coordinate systems.

It presents itself as an invariant consisting of tensor components of stress or strain and has the ability to take into account the difference between the resistances under tension and compression.

Regarding the plane stress state, the Tsai-Wu is presented in the most known form:

$$f_1\sigma_1 + f_2\sigma_2 + f_{11}\sigma_1^2 + f_{22}\sigma_2^2 + f_{66}\tau_6^2 + 2f_{12}\sigma_1\sigma_2 = 1 \quad (6)$$

The general coefficients for the quadratic failure criterion of Tsai-Wu are obtained through the application of elementary loadings on the ply.

$$f_1 = \frac{1}{S_{11}^+} - \frac{1}{S_{11}^-} \quad (7)$$

$$f_{11} = \frac{1}{S_{11}^+S_{11}^-} \quad (8)$$

$$f_2 = \frac{1}{S_{22}^+} - \frac{1}{S_{22}^-} \quad (9)$$

$$f_{22} = \frac{1}{S_{22}^+S_{22}^-} \quad (10)$$

$$f_{12} \cong -0,5(f_{11}f_{22})^{1/2} \quad (11)$$

The Tsai-Wu criterion is not capable of identifying the laminate failure mode. It includes all the stress components in the same equation which will determinate the failure of the ply according to the contribution of each component.

3.3 Hashin criterion

The Hashin criterion identifies four different modes of failure for the composite material: tensile fiber failure, compressive fiber failure, tensile matrix failure, and compressive matrix failure.

If $\sigma_{11} \geq 0$, the Tensile **Fiber** Failure Criterion is:

$$F_F^+ = \left(\frac{\sigma_{11}}{S_{11}^+}\right)^2 + \alpha \left(\frac{\sigma_{12}}{S_{12}}\right)^2 \geq 1.0 \quad (12)$$

If $\sigma_{11} < 0$, the Compressive **Fiber** Failure Criterion is:

$$F_F^- = \left(\frac{\sigma_{11}}{S_{11}^-}\right)^2 \geq 1.0 \quad (13)$$

If $\sigma_{22} \geq 0$, the Tensile **Matrix** Failure Criterion is:

$$F_m^+ = \left(\frac{\sigma_{22}}{S_{22}^+}\right)^2 + \left(\frac{\sigma_{12}}{S_{12}}\right)^2 \geq 1.0 \quad (14)$$

If $\sigma_{22} < 0$, the Compressive **Matrix** Failure Criterion is:

$$F_m^- = \left(\frac{\sigma_{22}}{2S_{23}}\right)^2 + \left[\left(\frac{S_{22}^-}{2S_{23}}\right)^2 - 1\right] \left(\frac{\sigma_{22}}{S_{22}^-}\right) + \left(\frac{\sigma_{12}}{S_{12}}\right)^2 \geq 1.0 \quad (15)$$

where:

S_{23} - Transverse shear strength, plane 2-3;

α - User-specified coefficient that determines the contribution of the longitudinal shear stress

to fiber tensile failure. Allowable range is $0.0 \leq \alpha \leq 1.0$, and the default value is $\alpha=0$.

4 Progressive damage

After the first ply failure, the composite material is able to resist an additional load as the load path is changed to intact plies. Computationally it is done through a progressive damage subroutine where a representation of the real damage is implemented in the simulation. All progressive damage is coded based in failure criteria, and the material properties are degraded when a specific condition is violated.

The progressive damage methods are summarized as mode-dependent and mode-independent. The mode-dependent criteria take into account what failure mode was achieved and degrades only the material properties related to this mode. The Hashin criterion and the Maximum Stress criterion are examples of mode-dependent failure criteria used to code progressive damage algorithms. On the other hand, the mode-independent progressive damage criteria do not take into account the failure mode, and degrades all mechanical properties of the material when the failure criteria is violated. These mode-independent methods input in the numerical model more damage, leading to premature failures and conservative results.

Computationally, the analysis is implemented in the following steps which are graphically presented in the flowchart in Figure 2:

1. The model is build: definition of mesh, material, boundary conditions and load, in this case applied through enforced displacement of the pin;
2. The analysis is segmented in an amount of steps that allow obtaining a good resolution of the mechanical behavior and the damage evolution;
3. The first increment step is executed and all stresses in on-axis orientation are calculated;
4. The failure criterion is evaluated for each element and each ply;
5. Each element-ply that violate the imposed conditions of the failure criterion has its material properties properly degraded according to the progressive damage subroutine;
6. The analysis continues to the next displacement step and this procedure continues until the entire displacement is imposed.

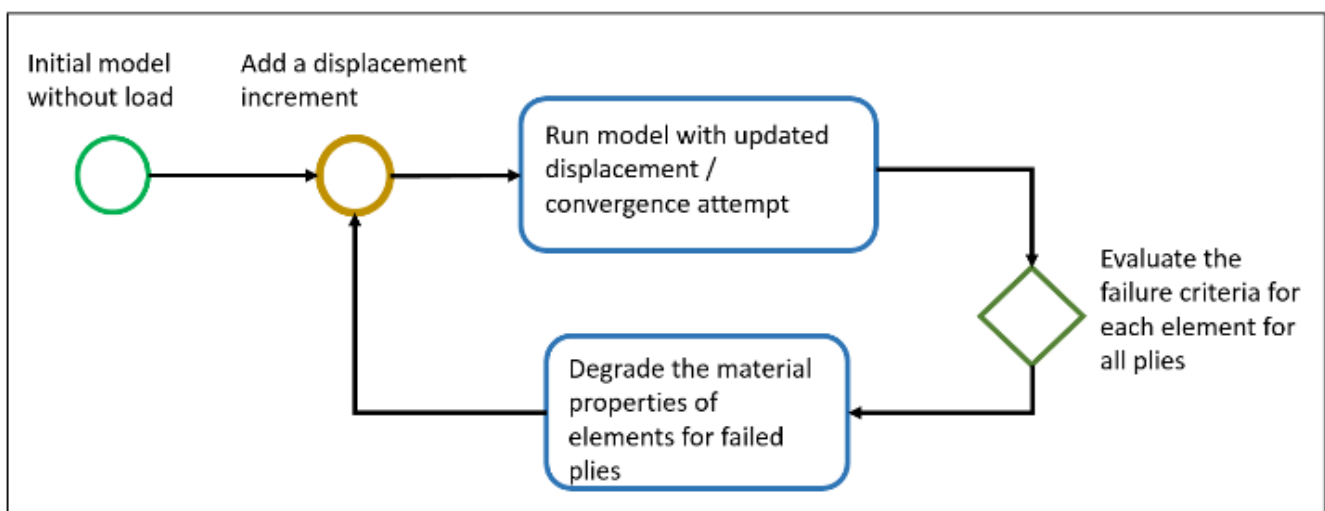


Fig. 2. Flowchart of progressive damage subroutine

The commercial software ABAQUS was used to run all the simulations. The progressive damage is implemented through a USDFLD subroutine. The damage degrades the elastic properties of a material through one or two damage variables (FV1, FV2) of interest in this work.

The USDFLD subroutine reads the output from previous step and updates the properties of the material for the element in the beginning of the actual step. This subroutine does not update the material properties in the element for the same step, which makes the choice of the increment size a sensible task, once this will reflect in the precision and resolution of the results for progressive damage. The lower the increment size, the better the results, but more computational time is required.

5 Methodology

The material used in this study is the pair finer/resin IM-7/PIXA (graphite fibers in polyimide resin) composite from Mitsui Chemicals Co. Ltd., presented as unidirectional prepreg plies. The lay-up configuration is quasi-isotropic with the following sequence: [+45/0/-45/90]_{2S}. Each one of the laminas has a thickness of 0.14 mm, resulting in a laminate with 2.24mm total thickness. Table 1 shows the properties of the unidirectional lamina.

Table 1 – Unidirectional ply properties [2]

Material properties	IM-7/PIXA
Longitudinal modulus, E_1 (GPa)	152.4
Transverse modulus, E_2 (GPa)	8.06
Shear modulus, G_{12} (GPa)	4.69
Longitudinal tensile strength, S_{11}^+ (MPa)	0.34
Longitudinal compression strength, S_{11}^- (MPa)	2293
Transverse tensile strength, S_{22}^+ (MPa)	948.2
Transverse compression strength, S_{22}^- (MPa)	210
In-plane shear strength, S_{12} (MPa)	155.3

The present work investigates how three of the most known failure criteria, (Hashin, Tsai-Wu and Maximum Stress) respond to bearing failure mode. Furthermore, the damage developed in

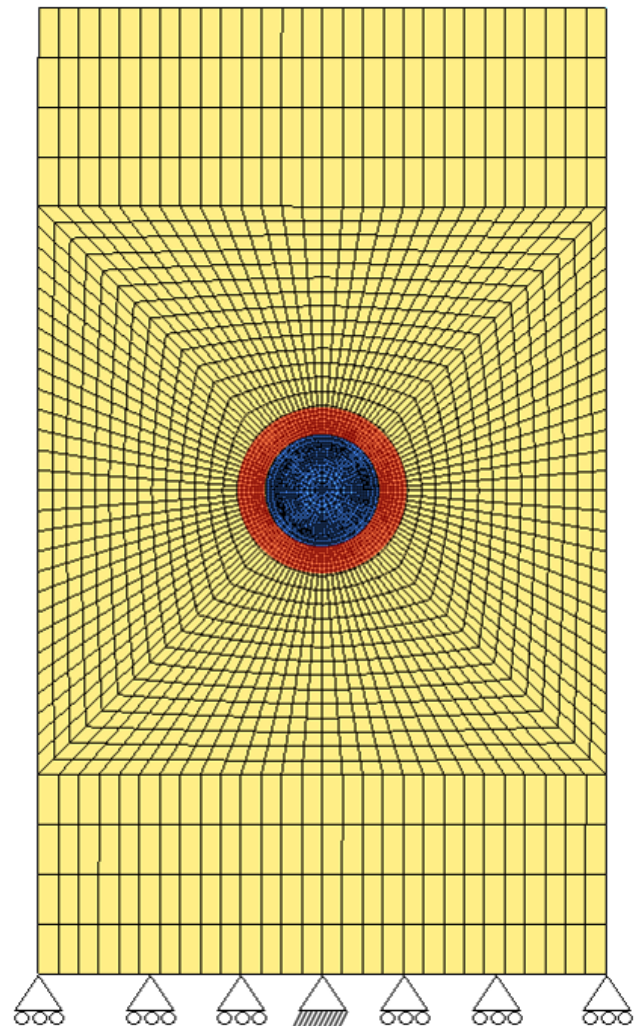


Fig. 3. Finite element model for analysis

each criterion is compared to experimental results in order to verify the accuracy of the simulations.

For composite connections failing in bearing, initial bearing failure typically occurs at 4% deformation of the hole diameter as recommended by ASTM D953-10 [10]. This value of 4% was adopted for this analysis.

For the analysis, two models were developed. For Tsai-Wu and Maximum Stress criteria, the problem was modeled with continuum shell elements. For Hashin criterion, a solid-element model was constructed in order to make it possible to obtain the out of plane shear stress component. The width to diameter ratio is $w/d=5$. This value was adopted following the suggestion of Ahmad *et al.* [11] who studied the influence of this ratio in failure mode. For a finger-tight bolt joint, the ratio w/d should be greater than 4 to

make the bearing mode dominant. In the presence of wrench torque, this ratio should be greater than 5. If the w/d ratio adopted is less than the values mentioned, the net-tension failure mode will arise earlier with stress levels considerably lower. The continuum shell model allows the use of surface contact between the pin and composite hole surface in ABAQUS.

The pin was modeled using solid elements with 6/32 in of diameter size. Its material is the metal alloy Ti-6Al-4V with Young’s modulus of 113.8 GPa and Poisson’s ratio of 0.342. The load application is made through the enforcement displacement of the pin.

Table 2 – Lay-up equivalent configuration for each rotation angle

Rotation angle	Lay-up
0°	[45/0/-45/90] _{2s}
22.5°	[67.5/22.5/-22.5/-22.5] _{2s}
45°	[90/45/0/-45] _{2s}
67.5°	[-22.5/67.5/22.5/-22.5] _{2s}
90°	[-45/90/45/0] _{2s}

The analysis was carried in five base directions related to initial configuration [45/0/-45/90]_{2s} as shown in Table 2. This approach has the

objective to obtain the material behavior due to other load direction, misalignment of the composite or uncertainties concerning the displacement direction of the pin.

The model configuration is shown in Figure 3. The blue region is the pin mesh; the yellow and red are the composite mesh. The region highlighted in red has a translational constraint in the normal direction to represent the washer.

The analysis was broken into two steps. The first step establishes the contact between surfaces of pin and composite hole. The second step continues where the first ended to generate the progressive damage of the structure along a sufficient number of increments.

The monitored analysis outputs are displacement and nodal force, stress in each ply and field state variables. From that monitoring it is possible to obtain the damage evolution and determinate the failure by bearing.

Tables 3 to 5 present the material properties respectively for Maximum Stress, Hashin and Tsai-Wu criteria, for the specific failure condition.

Table 3. Maximum Stress criterion material properties for each state. $D_{MS}=0.1$

Maximum Stress criterion	E ₁	E ₂	v ₁₂	G ₁₂	G ₁₃	G ₂₃	FV ₁	FV ₂
Intact	E ₁	E ₂	v ₁₂	G ₁₂	G ₁₂	G ₂₃	0	0
Matrix failure	E ₁	D _{MS} E ₂	0	D _{MS} G ₁₂	D _{MS} G ₁₂	D _{MS} G ₂₃	0	1
Fiber breakage	D _{MS} E ₁	E ₂	0	D _{MS} G ₁₂	D _{MS} G ₁₂	D _{MS} G ₂₃	1	0
Matrix and fiber failure	D _{MS} E ₁	D _{MS} E ₂	0	D _{MS} G ₁₂	D _{MS} G ₁₂	D _{MS} G ₂₃	1	1

Table 4. Hashin criterion material properties for each state. $D_H=0.3$

Hashin criterion	E ₁	E ₂	v ₁₂	G ₁₂	G ₁₃	G ₂₃	FV ₁	FV ₂
Intact	E ₁	E ₂	v ₁₂	G ₁₂	G ₁₂	G ₂₃	0	0
Matrix failure	E ₁	D _H E ₂	0.1*D _H v ₁₂	D _H G ₁₂	D _H G ₁₂	D _H G ₁₃	1	0
Fiber breakage	D _H E ₁	D _H E ₂	0.1*D _H v ₁₂	D _H G ₁₂	D _H G ₁₂	D _H G ₁₃	0	1
Matrix and fiber failure	D _H E ₂	D _H E ₂	0.1*D _H v ₁₂	D _H G ₁₂	D _H G ₁₂	D _H G ₁₃	1	1

Table 5. Tsai-Wu material properties for each state. $D_{TW}=0.1$

Tsai-Wu criterion	E ₁	E ₂	v ₁₂	G ₁₂	G ₁₃	G ₂₃	FV ₁
Intact	E ₁	E ₂	v ₁₂	G ₁₂	G ₁₂	G ₂₃	0
Failure	D _{TW} E ₁	D _{TW} E ₂	0	D _{TW} G ₁₂	D _{TW} G ₁₂	D _{TW} G ₁₃	1

6 Results

For the Hashin and Tsai-Wu failure criteria, cases with rotation of the laminate were simulated to observe the mechanical response of quasi-isotropic configuration under bearing load. The results, presented in Figures 4 and 5 respectively for Hashin and Tsai-WU, show that even for large displacement and a lot of accumulated structural damage, the joint strength predicted with Hashin failure criterion (7.8 kN) is 20% higher than Tsai-Wu results (6.5 kN) for a quasi-isotropic lay-up.

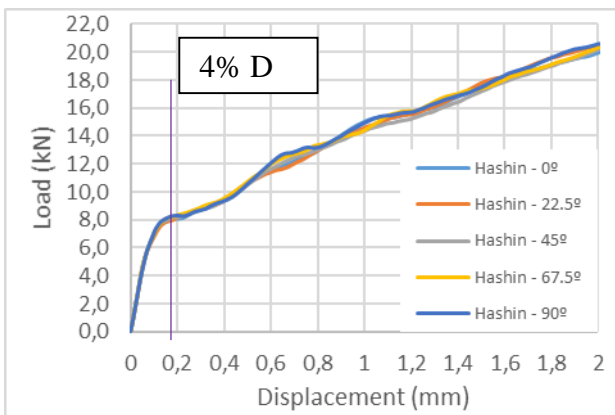


Fig. 4. Hashin Load Bearing for each angle rotation

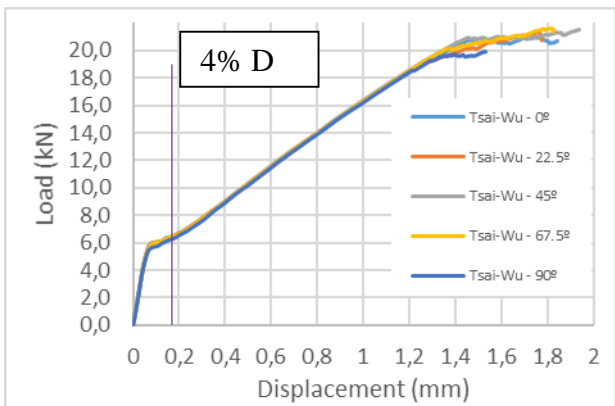


Fig. 5. Tsai-Wu Load Bearing for each angle rotation

Comparing the numerical results with the experimental data [3], it is noted a higher initial stiffness for all three failure criteria, but they reach the first knee in the Figure 9 before the experimental curve. This could be explained due to the model incapacity of taking into account the phenomenon of kinking band that would delay the knockdown of the material properties.

For the bearing failure, defined as 4% (0,195mm) deformation of the hole diameter, the experimental data presented higher strength. At this point, the Hashin (7.8 kN) and Maximum Stress (7.6 kN) criteria have very close load bearing allowable. On the other hand, the Tsai-Wu criterion gives the lower results (6.5 kN).

As the pin continue moving, the load bearing for all failure criteria continues to rise, but the experimental data suffer successive drops, and become softer. These failure criteria cannot give a reliable load bearing allowable for large deformations, higher than 10%.

The curve that had better approximation of the experimental data was the one from Hashin failure criterion, until 15% of hole deformation. The Tsai-Wu curve rises with a constant slope until reach a plateau, and the Maximum Stress simulations lost convergence closer than 1,1mm of hole elongation. As shown in the following pictures (Figures 6 to 8), the damage in the structure using was severe in the Maximum Stress case. The Hashin was the one with the less damage in the matrix++. The 0° ply suffered the largest damage from all plies in extension from hole surface.

The previous simulations were executed with w/d ratio instructed by Ahmad *et al.* [11], which is five. The experimental specimen has a w/d ratio of eight, and simulations were conducted with this ratio to verify possible divergences.

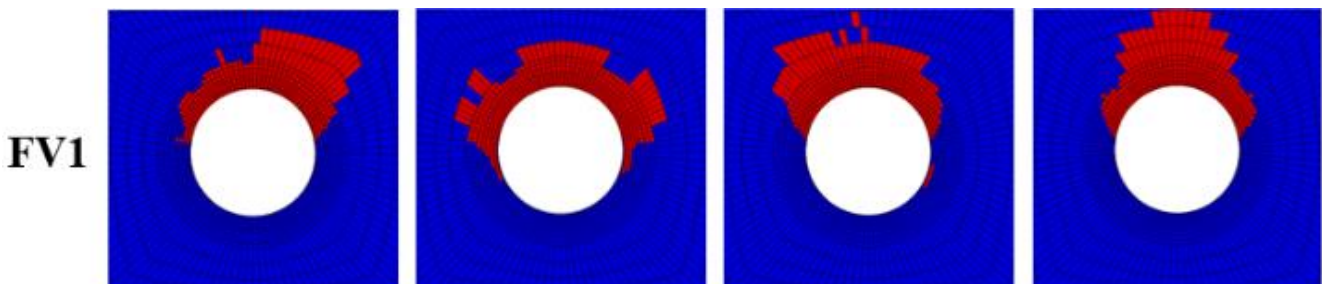


Fig. 6. Damage at 4%D – Tsai-Wu criterion

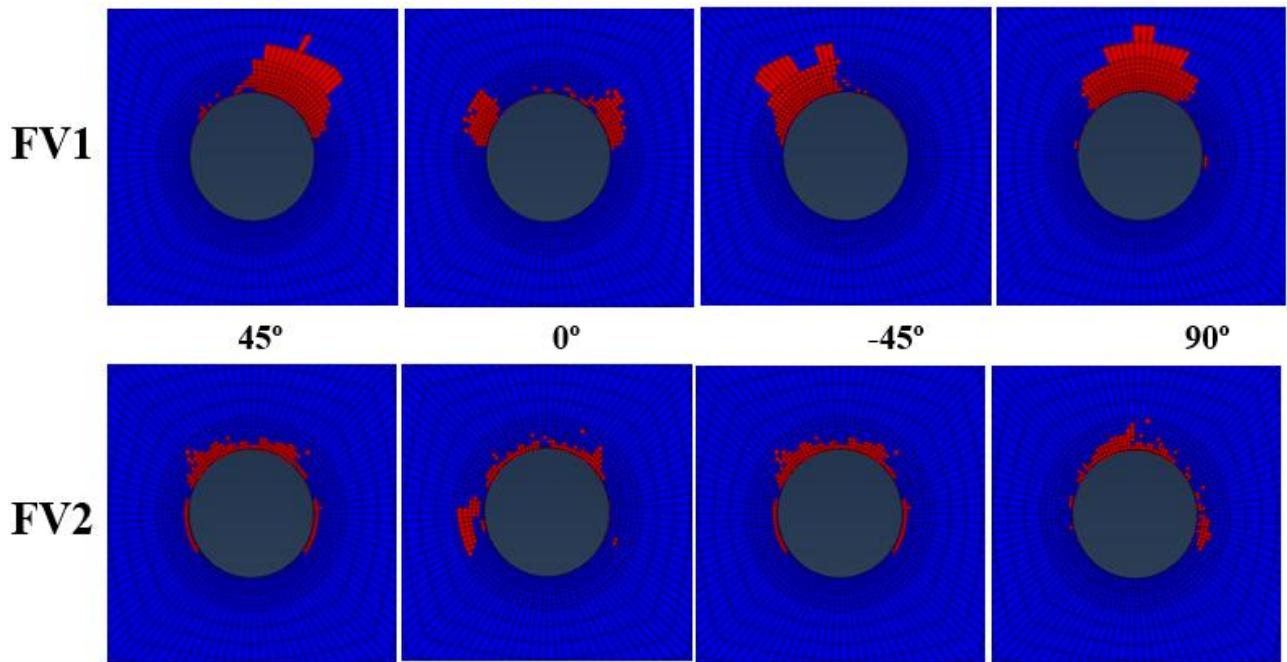


Fig. 7. Damage at 4%D – Hashin criterion

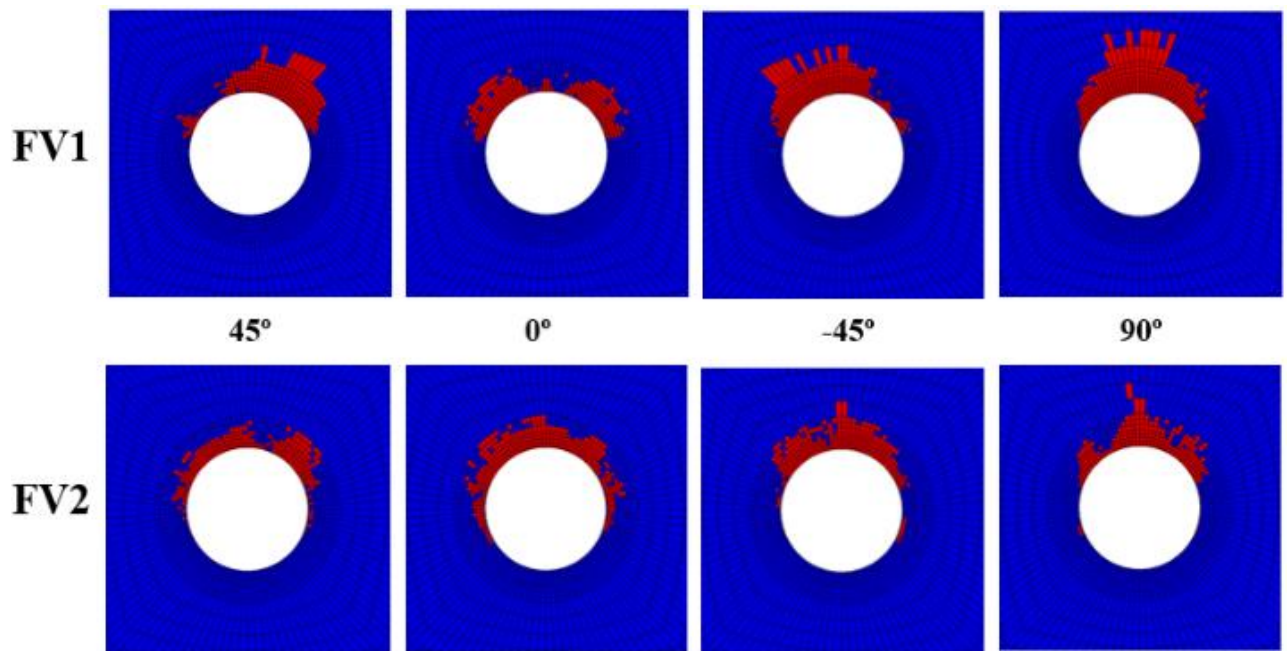


Fig. 8. Damage at 4%D – Maximum Stress criterion

For simulations with $w/d=8$ until 10% (0,635mm) of hole deformation the failure criteria chosen results in lower load at the pin (Figure 10) relative to experimental data, what gives conservative bearing allowable. The main divergence in the results for $w/d=8$ is concerned to mechanical behavior for Hashin

failure criterion after the first knee, where besides de conservative values, the curve has a similar slope compared to experimental information.

It was noted that for $w/d=5$ models the damage spread quickly for the material outside the washer region after the bearing failure (4% D).

For the $w/d=8$ the damage remains in the region close to the hole for a higher load compared to $w/d=5$. From this and the mechanical response divergence previous exposed, a size influence related to specimen width were noted, inserting other failure mode to the simulation.

7 Conclusion

From the results presented in this work, the three selected failure criteria cannot represent the mechanical behavior of the structure with reliability. In small deformations, the failure criteria adopted give conservative results, but for large deformations on bearing load, they give bearing allowables that are not safe for design. For the quasi-isotropic composite layup studied, the misalignment of the load direction in the plane of the composite has a negligible effect in the mechanical behavior under bearing load. It was noted a size influence related to specimen width in obtaining a pure bearing failure mode in the simulations, what recall to a suitable choice for model size. There are other phenomena that occur in the material during the bearing process, like kinking bands, delaminations, and other 3D effects that need be accounted to achieve a more reliable model.

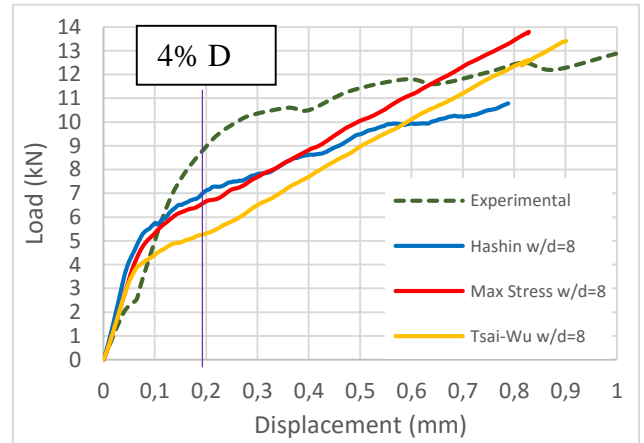


Fig. 10. Results for $w/d=8$ simulations. Experimental data from [2]

8 References

- [1] Y. Xiao, W. Wang, Y. Takao e T. Ishikawa, "The effective friction coefficient of a laminate composite, and analysis of pin-loaded plates," *J Compos Mater*, vol. 34, pp. 69-87, 2000.
- [2] Y. Xiao and T. Ishikawa, "Bearing strength and failure behavior of bolted composite joints (part II: modeling and simulation)," *Composites Science and Technology*, vol. 65, pp. 1032-1043, 2005.

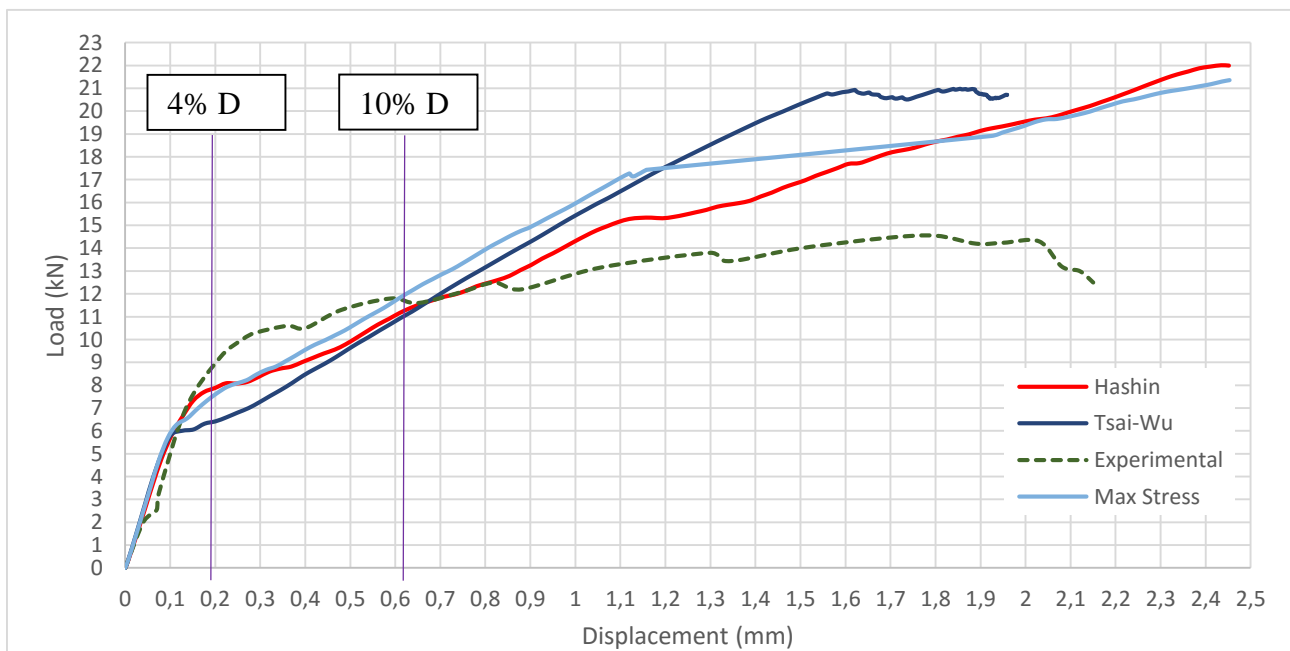


Fig. 9. Results for $w/d=8$ simulations. Experimental data from [2]

- [3] Y. Xiao and T. Ishikawa, "Bearing strength and failure behavior of bolted composite joints (part I: Experimental investigation)," *Composites Science and Technology*, vol. 65, pp. 1022-1031, 2005.
- [4] F. Ascione, L. Feo and F. Maceri, "An experimental investigation on the bearing failure load of glass fibre/epoxy laminates," *Composites: Part B*, vol. 40, pp. 197-205, 2009.
- [5] K. C. Warren, R. A. Lopez-Anido e J. Goering, "Behavior of three-dimensional woven carbon composites in single-bolt bearing," *Composite Structures*, vol. 127, pp. 175-184, 2015.
- [6] M. Nakayama, N. Uda, K. Ono, S.-i. Takeda e T. Morimoto, "Design-oriented strength of mechanical joints in composite laminate structures and reliability-based design factor," *Composite Structures*, vol. 132, pp. 1-11, 2015.
- [7] C. Sola, B. Castanié, L. Michel, F. Lachaud, A. Delabie e E. Mermoz, "On the role of kinking in the bearing failure of composite laminates," *Composite Structures*, vol. 141, pp. 184-193, 2016.
- [8] M. McCarthy, V. Lawlor, W. Stanley e C. McCarthy, "Bolt-hole clearance effects and strength criteria in single-bolt, single-lap, composite bolted joints," *Composites Science and Technology*, vol. 62, pp. 1415-1431, 2002.
- [9] Z. Kapidžić, L. Nilsson and H. Ansell, "Finite element modeling of mechanically fastened composite-aluminum joints in aircraft structures," *Composite Structures*, vol. 109, pp. 198-210, 2014.
- [10] ASTM D953-10, "Standard Test Method for Bearing of Plastics," ASTM International, 2010.
- [11] H. Ahmad, A. Crocombe e P. Smith, "Strength prediction in CFRP woven laminate bolted double-lap joints under quasi-static loading using XFEM," *Composites: Part A*, vol. 56, pp. 19-202, 2014.

9 Acknowledgements

Authors would like to acknowledge the support from FAPEMIG, CAPES and CNPq.

10 Contact Author Email Address

Euler S. Dias: euler.samuel@gmail.com

Carlos A. Cimini Jr.: carlos.cimini@gmail.com

Copyright Statement

The authors confirm that they, and/or their company or organization, hold copyright on all of the original material included in this paper. The authors also confirm that they have obtained permission, from the copyright holder of any third party material included in this paper, to publish it as part of their paper. The authors confirm that they give permission, or have obtained permission from the copyright holder of this paper, for the publication and distribution of this paper as part of the ICAS proceedings or as individual off-prints from the proceedings.